Identification of deep magnetized structures in the tectonically active Chlef area (Algeria) from aeromagnetic data analyzed with 2-D and 3-D imaging derived from the wavelet and ridgelet transforms

H. Boukerbout, A. Abtout, Dominique Gibert, B. Henry, B. Bouyahiaoui, M.E.M. Derder

▶ **To cite this version:**

H. Boukerbout, A. Abtout, Dominique Gibert, B. Henry, B. Bouyahiaoui, et al.. Identification of deep magnetized structures in the tectonically active Chlef area (Algeria) from aeromagnetic data analyzed with 2-D and 3-D imaging derived from the wavelet and ridgelet transforms. Journal of Applied Geophysics, 2018, 154, pp.167-181. 10.1016/j.jappgeo.2018.04.026 . insu-01785456

HAL Id: insu-01785456
https://insu.hal.science/insu-01785456

Submitted on 4 May 2018

HAL is a multi-disciplinary open access archive for the deposit and dissemination of scientific research documents, whether they are published or not. The documents may come from teaching and research institutions in France or abroad, or from public or private research centers.

L'archive ouverte pluridisciplinaire **HAL**, est destinée au dépôt et à la diffusion de documents scientifiques de niveau recherche, publiés ou non, émanant des établissements d'enseignement et de recherche français ou étrangers, des laboratoires publics ou privés.

Accepted Manuscript

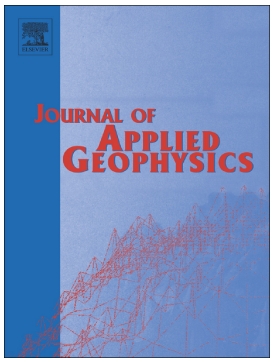

Identification of deep magnetized structures in the tectonically active Chlef area (Algeria) from aeromagnetic data analyzed with 2-D and 3-D imaging derived from the wavelet and ridgelet transforms

H. Boukerbout, A. Abtout, D. Gibert, B. Henry, B. Bouyahiaoui, M.E.M. Derder

PII: S0926-9851(16)30688-7
DOI: doi:10.1016/j.jappgeo.2018.04.026
Reference: APPGEO 3509

To appear in:

Received date: 21 December 2016
Revised date: 27 January 2018
Accepted date: 27 April 2018

Please cite this article as: H. Boukerbout, A. Abtout, D. Gibert, B. Henry, B. Bouyahiaoui, M.E.M. Derder , Identification of deep magnetized structures in the tectonically active Chlef area (Algeria) from aeromagnetic data analyzed with 2-D and 3-D imaging derived from the wavelet and ridgelet transforms. The address for the corresponding author was captured as affiliation for all authors. Please check if appropriate. Appgeo(2017), doi:10.1016/j.jappgeo.2018.04.026

This is a PDF file of an unedited manuscript that has been accepted for publication. As a service to our customers we are providing this early version of the manuscript. The manuscript will undergo copyediting, typesetting, and review of the resulting proof before it is published in its final form. Please note that during the production process errors may be discovered which could affect the content, and all legal disclaimers that apply to the journal pertain.

ACCEPTED MANUSCRIPT

Identification of deep magnetized structures in the tectonically active Chlef area (Algeria) from aeromagnetic data analyzed with 2-D and 3-D imaging derived from the wavelet and ridgelet transforms.

H. Boukerbout[1*], A. Abtout[1], D. Gibert[2], B. Henry[3], B. Bouyahiaoui[1] and M.E.M Derder[1].

[1]Centre de Recherche en Astronomie, Astrophysique & Géophysique-Observatoire d'Alger. Alger. Algeria

[2]Géosciences Rennes, CNRS/INSU (UMR 6118) & Université Rennes1, Rennes, France

[3]Institut de Physique du Globe Paris. Sorbonne Paris Cité Univ. Paris Diderot & UMR 7154 CNRS. Saint Maur des Fossés. France.

*Corresponding author: H. Boukerbout. Phone numbers: +213 771 425 880; +213 21 90 44 54. Fax: +213 21 90 44 59.e-mail address: s.boukerbout@craag.dz

Abstract

The Chlef region constitutes a key area to study neotectonics structures and their geodynamical context. Aeromagnetic data analyzed using different processing methods (shaded relief technique, computation of vertical gradient, upward continuation, use of the continuous wavelet transform and ridgelet transform), allow establishing a structural image of emerging and deep structures both onshore and offshore. Magnetic anomalies, over the Mediterranean Sea, the Chlef basin and the Ouarsenis Mounts, are well-correlated with the known geological structures. Long and short wavelength anomalies have been distinguished. The short wavelength anomalies are associated with the volcanic rocks on the coast from Chenoua to El Marsa and with the basement in the Boukadir zone in the sedimentary Chlef basin. The long wavelength anomalies to the South are associated mainly with deep E-W

ACCEPTED MANUSCRIPT

structures, limiting the Chlef basin. To the North, similar structures have been identified in the Mediterranean Sea. The compilation of the identified magnetic features leads to geometrical shape corroborating the structure in blocks of the Chlef basin.

Keywords:

Aeromagnetic data, Chlef, wavelet transform, ridgelet transform, 2D - 3D imaging, deep magnetized structures.

1. Introduction

The Chlef region (Figure 1) is located in North of Algeria around coordinates: 00°33'- 02°00'E & 35°48'- 36°56'N. It is one of the most seismically active zones of the western Mediterranean Sea (Meghraoui et al., 1996; Bezzeghoud et al., 1995; Yelles et al., 2006) related to the collision between African and European plates since the Upper Cretaceous (Dewey et al., 1989; Le Pichon et al., 1988; Ricou, 1994). Kinematic models based on the study of the magnetic anomalies in the Atlantic Ocean; showed that this convergence is related to a counter clockwise rotation of Africa with respect to Eurasia (Dewey et al., 1989; Mazzoli and Hetman, 1994; Rosenbaum et al., 2002). The seismic activity in this area is directly associated with the plate boundary between Europe and Africa. This region was affected by two very destructive seismic events: the 1954 9th September Orleansville earthquake with a 6.5 magnitude and the El Asnam one of 1980 10th October (7.3 magnitude) (Karnik, 1969; Dewey, 1991). Studies of structural geology, seismicity and seismotectonics were therefore strongly developed in this region to better understand the presently active deformation mechanisms (e.g. Rothé, 1950; Perrodon, 1957; Tapponier, 1977; Girardin et al., 1977; Philip, 1983; Thomas, 1985; Ouyed, 1981; Meghraoui, 1988; Yielding et al., 1989;

ACCEPTED MANUSCRIPT

Bufforn et al., 1995; Idres et al., 1996; Lammali et al., 1997; Ydri, 1988; Idres et al., 1998; Boukerbout and Abtout, 2000; Domzig et al., 2006; Aifa and Zaagane, 2014; Abtout et al., 2014).

With the same purpose, the aeromagnetic data supply further information on the causative geological structures of the magnetic anomalies. The use of methods developed recently such as the wavelet and the ridgelet transforms, applied to process the magnetic field data, allows establishing 2-D and 3-D images of the geological bodies both at surface and at depth as well inshore as offshore.

The present study is a contribution in a large project including geophysical and geological surveys in the Chlef region (CMEP Project 08MDU752). The main objectives of this study are to identify the geometry of the major tectonic contacts bounding the Chlef basin, to evaluate the depth of the different identified structures and to have a better knowledge of the basin basement. Geophysical methods and particularly aeromagnetic approach are adapted for obtaining a realistic model of the deep tectonic structures. This work leads to 2D and 3D representation from a set of sections across the geological units and magnetic field anomalies, to the geometric relationships existing between the different geological features. It also provides additional information enabling for example geologists to refine the structural interpretation of the volcanic domains and then improving the knowledge of the studied region.

Figure 1.

ACCEPTED MANUSCRIPT

2. Geological setting

The studied region (Figure 1) includes a large area from Mediterranean Sea to the North to the Ouarsenis Mountains to the South. Its central part is an intra mountainous depression of the Tellian chain: the post-nappes Chlef basin. This basin is filled by Mio-Plio-Quaternary rocks, lying on ante-Neogene basement. The latter outcrops as flyshoid and epi-metamorphic massifs, like Temoulga and Doui. These massifs are mainly composed of Siluro-Devonian schistosed limestones with a Jurassic dolomitic limestones cover (Kireche, 1977). The basin has an elongated shape, suggesting compressional movements (Meghraoui et al., 1986) related to the Alpine orogeny (Perrodon, 1957). The neo-tectonics studies show that the main deformation is a NNW-SSE compression giving overthrusting reverse and strike-slips faults (Groupe de Recherche néotectonique de l'arc de Gibraltar, 1977; Philip and Thomas, 1977) related to African and European plate movements (Philip and Thomas, 1977; Minster and Jordan, 1978; Anderson and Jackson, 1987).

Volcanic activity in the basin is evidenced by stratified cineretic deposits of upper Miocene age in the SW of the studied area (Perrodon, 1957), a small rhyolitic outcrop (0°35'E, 36°05'N), microgranite dykes cutting the upper Miocene deposits in the Dahra (Anderson, 1936) and biotitic andesites in the Beni-Chougrane.

Along the coast, east of Tenes, rhyolites and andesitic dacites (Hernandez and Lepvrier, 1976) have ages varying between 15 and 9 Ma. The calc-alkaline volcanism is known all over the coastal border of the northern Tell in a band parallel to the coast line. It might evidence an ancient subduction zone (Girod and Girod, 1977, Maury et al., 2000). These volcanic episodes would occur between lower Miocene compressional phases related to the formation of the nappes (Mattauer, 1958; Delteil, 1974) and the Plio-Quaternary compression. This situation is probably due to a period where local relaxation of compressional stresses allows volcanic

ACCEPTED MANUSCRIPT

eruptions. More to the West, the volcanic activity was continuous during the Plio-Quaternary in contrast to its absence in the Chlef basin (Bellon and Guardia, 1980). Nevertheless E-W extensional movements may be simultaneous to the N-S compression (Bousquet and Philip, 1981) that is the main deformation mechanism during the Plio-Quaternary period in the western Tellian Atlas (Thomas, 1974; Philip and Thomas, 1977; Meghraoui, 1982). Therefore, the Plio-Quaternary alkaline volcanic manifestation west of the Chlef basin, likely does not characterize an independent extensional episode.

At a local scale, remarkable tectonic structures can be observed across the basin.

- The Sara El Marouf broken fold correspond to the El Asnam fault, reactivated during the October 10, 1980, El Asnam earthquake (Ouyed et al., 1981; King and Vita Finzi, 1981). It has a NE-SW direction and it is limited to the SE by a reverse active fault since the early Quaternary (Meghraoui, 1982, 1986). It crosses the eastern part of the basin separating the Oued Fodda valley from El Asnam valley.

- The Boukadir broken fold is located about 40 km in the WSW of El Asnam, separating the El Asnam valley from Relizane valley. The Boukadir fault shows recent activity affecting Quaternary deposits. It corresponds to a thrust striking N065 with a NW.

- A third structure crossing the basin is the Dahra fault, which separates the Relizane valley from the Mostaganem valley. It affects Quaternary deposits that are strongly deformed, clearly evidencing an active flexure.

- The southern limit of the basin which is the southern limit of the Quaternary sediments is defined by a tectonic linear contact between recent Quaternary silts and upper Miocene limestones. Its strike is N070 and it runs for some 150km from El Asnam to Relizane (Meghraoui et al., 1986).

ACCEPTED MANUSCRIPT

3. Aeromagnetic data

The aeromagnetic map used in this study outcome from the airborne survey which cover Algeria during the period from 1970-1974 by Aero Service Corporation, at a constant flight altitude of 150m along N20W lines 2km apart with perpendicular tie-lines at 5 km intervals; sampling distance along the profiles was about 46m. The survey data were originally recorded in analogue form (Paterson et al., 1976). The digital dataset used for this study was obtained by digitizing the paper map each 2nT contour line at a scale of 1/200,000. The digitizing method is based on recognition of shape. There is no spatial error introduced in the automated vectorization process. The vector data is faithfully reproduced in vector form. 1871 points were obtained. The survey was then processed to compute magnetic anomaly map through the subtraction of a normal field, hereby established for the period of the airborne survey (Boukerbout and Abtout, 2010), by the use of Algerian repetitive network data. The values cover the area at coordinates: “00°33’- 02°00’E” & “35°48’- 36°56’N” and are interpolated to a spacing regular grid of 325m x 325m. Each grid node holds a calculated value of the field. The scattered magnetic data were interpolated onto grid using the nearest neighbour interpolation technique. This method seeks to generate the smoothest surface which closely reproduces the observed data.

4. Processing and interpretation of aeromagnetic field maps

Because of the inclination of about 54° of the magnetic field at latitude of survey for the period of 1974, there is a slight discrepancy between the magnetic anomalies and the corresponding causative magnetized bodies. In order to replace the anomalies above their geological sources, the magnetic anomaly map was reduced to the pole. For this purpose, we

ACCEPTED MANUSCRIPT

need to know, the values of inclination and declination of normal earth's field *(In, Dn)* and those of the magnetization *(Im, Dm*). The difficulty is to determine *Im* and *Dm*. From measurements made on 73 samples from the andesites in the studied area, Idres and al. (1998) point out that remnant magnetization is negligible (Derder et al., 2013), so only the induced magnetization is taken account, therefore, the used parameters of the magnetization were the same that the ones of normal field (54° for the inclination and -4° for the declination). The aeromagnetic map reduced to the pole (Figure 2) is not very different in shape and amplitude from the original map. The reduced map shows a slight northward offset of the magnetic anomalies, an increase in the amplitude of the positive magnetic anomalies and an attenuation of the negative ones.

The long wavelength magnetic anomalies can be separated from the short wavelength ones by calculating an upward continuation at different altitudes, for instance, we choose to show the upward continued by 5 km (Figure 3).

To highlight the short wavelength anomalies that reflect the signature of superficial or sub outcropping geological structures, we use the" technique of shading relief" (Mc Donald et al., 1992). This technique consists in representing the magnitude of the field as shades of gridded data. Produced images are obtained by treating the image as a topographic surface and simulating illumination either by using a simple mathematical model or by filtering the image to create a shaded relief image. Shaded relief image convey changes in values and do not contain any information on the magnitude of the field. This is particularly useful for enhancing subtle linear features which maybe related to geological structures (Mc Donald et al., 1992). The shading relief technique is applied to the reduced to pole anomaly map illuminated from the northeast, to show up the short wavelength of the magnetic anomalies and enhance features with a northwesterly trend (Figure 4). The advantage of this method: it

ACCEPTED MANUSCRIPT

doesn't modify the strength of the high frequency signature, but as the illumination is directional, some anomalies may be unfavourably illuminated and thus not show up.

We also use the technique of calculating gradient of magnetic anomalies: it has no directional bias but by amplifying the short wavelengths and attenuating the long wavelengths, it can produce some oscillations which can have effect of distorting the legibility and may be lead to erroneous interpretations. The vertical gradient map is shown in Figure 5.

Figures 2, 3, 4 and 5.

5. Description of the aeromagnetic field maps

The examination of different magnetic maps shows that the strongest anomalies are those located in the North: all along the coast deriving from volcanic formations and in the Mediterranean Sea but, also in the Chlef basin and in the South part of the studied area. A set of N80E positive magnetic anomalies occurs between Gouraya and Tenes and follows the coast. This set is made up of a series of short wavelength anomalies (Figures 4 and 5) that arise over a group of calc-alkaline volcano formations but coincide with no precise geological boundary. In addition, these small anomalies contain a number of small offsets that reflect strike-slip-faults (Schettino and Turco, 2006; Domzig et al., 2006; Yelles et al., 2009; Leprêtre et al., 2013). In Northward of this set, a large and intense magnetic anomaly, trending E-W, occurs offshore. The feature giving rise to this anomaly may be buried very deep. It can be shown on upward extensions maps at different altitudes (Figure 3), whereupon this magnetic anomaly remains very strong indicating a relatively deep rooting, whereas those derived from the signature of the basin disappear between altitudes of 4 and 5 km, indicating that the basin is not flat with a mean thickness of 5 km. However the overview

ACCEPTED MANUSCRIPT

of all processed maps show that the magnetized structure is not simple and will reflect the geological complexity of the studied area.

The anomalies on the magnetic map (Figure 2) are correlated to geological data (Figure 1); they correspond, in the West part of the studied area, to bodies within the Chlef basin. The Boukadir positive magnetic anomaly is made up of two lobes disrupted by a discontinuity in the NW-SE direction. This anomaly may correspond to a succession of basaltic sills embedded between the calcareous formations (Aït Hamou, 1987; Meghraoui, 1988; Idres et al., 1998). In a northward, there is a negative magnetic anomaly corresponding to the Ouled Fares anticline. This anomaly could be produced by a magnetized source located at the boundary substratum-basin or by a succession of basic sills deeply rooted (Idres et al., 1998).

In the East of the region, there are two positive magnetic anomalies and one negative in their North appears. This magnetized substratum limits the Chlef basin in the South. The positive anomaly in the East is identified on the Doui massif, which is better defined.

The Chlef basin is composed of mio-Pliocene and quaternary formations lying on ante-Neogene basement. According to the compressional phase from Pliocene to Quaternary (Meghraoui, 1988), this substratum is outcropping in some places such as Temoulga, Rouina and Doui, in the form of epi-metamorphic and Jurassic massifs of different sizes. This outcropping basement is made up of Mesozoic and Palaeozoic formations. The Palaeozoic formations are composed of a metamorphic substratum over which lies a volcanic complex composed from lavas and tuffs. The Mesozoic formations are composed of Triassic and Cretaceous structures (Kirèche, 1977).

The long wavelength positive anomalies were probably caused by structures located in the recognized outcropping Palaeozoic substratum which limit the basin in South, since they are not superimposed on known outcropping Jurassic massifs. On the other hand, the long

ACCEPTED MANUSCRIPT

wavelength negative anomaly is located over the outcropping Jurassic massifs of Temoulga and Rouina. As this anomaly remains negative, its origin is in the Palaeozoic substratum which is more magnetized and deepest than the Cretaceous one. This is also confirmed by the identification of the sources of the magnetic anomalies in 2-D along the profile and in 3-D (see section 6, below) and by the gravity study of the same area (Idres et al., 1998; Abtout et al., 2014)

Some contacts are identified on the gradient map (Figure 5). The NW-SE one is thrusting in the sinistral way the Boukadir anomaly. The second one is perpendicular to the first and is identified in the South of the Boukadir anomaly. It shows the SW limit of the Chlef basin and the Palaeozoic substratum located in the South. It coincides with a part of the Relizane Fault. More in the North of this latter, two contacts appear and may be correspond to some deep aftershocks of El Asnam and Relizane Faults as they are parallel. In the East, between the negative magnetic anomaly and the positive one, appears a contact which may be correspond to the Palaeozoic substratum known in the South and which becomes more deepest in the North.

6. Identification of magnetic anomalies causative bodies with the continuous wavelet transform

The main application in geophysical potential fields studies is to identify the geological structures responsible of the anomalies by quantifying their depth, inclination, dip, geometry, and so on. These characterization and localization of the sources of geophysical potential fields anomalies lead to development of refined inversion and analysis techniques. Among these developed methods, the continuous wavelet transform (Grossmann and Morlet, 1984) which assists automatic interpretation of large amount of potential fields data, through many

ACCEPTED MANUSCRIPT

applications such as in filtering or inversion (Fedi and Quarta, 1998; Ridsdill-Smith and Dentith, 1999; Trad and Travassos, 2000; Boschetti et al., 2001; Leblanc et al., 2001; Li and Oldenburg, 2003).

In this study, we use methods based on the continuous wavelet transform to identify and localize the causative bodies of magnetic anomalies. The wavelet transform uses the property of the homogeneity degree of the analyzed function which allows detecting and characterizing homogeneous singularities in signals (Grossmann et al., 1987; Holschneider, 1988; Mallat and Hwang, 1992). This technique is described and detailed by Alexandrescu et al. (1995, 1996) with an application to geomagnetic time series. The wavelet theory can be found in the book of Holshneider (1995) and the theory of its application to potential fields data can be found in Moreau et al., (1997, 1999), Hornby et al., (1999), Sailhac et al., (2000), Sailhac and Gibert (2003), Boukerbout and Gibert (2006), Sailhac et al., (2009), Fedi et al., (2010), Fedi and Cascone (2011) and so on. Many studies illustrate application of this method, for instance we can refer to applications to aeromagnetic and magnetic data (Sailhac et al., 2000; Pouliquen and Sailhac, 2003; Boschetti et al., 2004; Vallée et al., 2004; Yang et al., 2010), electromagnetic data (Boukerbout et al., 2003), spontaneous electrical potential (Gibert and Pessel, 2001; Sailhac and Marquis, 2001, Saracco et al., 2004, Gibert and Sailhac, 2008; Mauri et al., 2010) and gravity data (Martelet et al., 2001; Fedi et al., 2004; Cooper, 2006; Chamoli et al., 2011; Abtout et al., 2014).

The 1-D continuous wavelet transform, $w[g,\phi_0](b,a)$ of a function $\phi_0(x\in\Re)$ is defined as convolution product (Grossmann and Morlet, 1984; Grossmann et al., 1985)

$$w[g,\phi_0](b,a)\equiv\int_{\Re}\frac{1}{a}g\left(\frac{b-x}{a}\right)\phi_0(x)dx=(D_a g*\phi_0)(b) \qquad \textbf{(1)}$$

ACCEPTED MANUSCRIPT

Where the function $g(x)$ is called the analyzing wavelet, $a \in \Re^+$ is the dilation parameter, b is the translation parameter, and the dilation operator D_a is defined by the following action (Goupillaud et al., 1984),

$$D_a g(x) \equiv \frac{1}{a} g\left(\frac{x}{a}\right) \tag{2}$$

In the case of 2-D potential fields anomaly data measured in the horizontal plane, the 1-D wavelet transform given by equation (1) may be generalized to give ridgelet transform (Candès, 1998; Candès and Donoho, 1999),

$$R[r,\phi_0](b,a,s_\perp) = \int_{\Re^2} \frac{1}{a} r\left(\frac{b-x}{a}, y, s_\perp\right) \phi_0(x,y)\,dx\,dy = \int_{\Re} \frac{dx}{a} g\left(\frac{b-x}{a}\right) \int_{\Re} \phi_0(x,y)\,dx\,dy$$

$$= W[g, RT[\phi_0, s_{//}]](b,a) \tag{3}$$

where $s_\perp$ is a unit vector perpendicular to the anomaly strike, $s_{//}$ is a unit vector in the direction of the elongated anomaly, the analyzing ridgelet is obtained by steering a 1-D Poisson wavelet $g(x)$ in the perpendicular direction y, RT is the Radon transform of the potential field anomaly. Equation (3) shows that the ridgelet transform of 2-D anomalies is given by the 1-D wavelet transform applied in the Radon domain. In practice, this is done by computing a 1-D wavelet transform for each direction in the Radon domain.

Explicitly the extension of the method in 3-D is to add an angular parameter in the wavelet domain by using the ridgelet transform which consists in a Radon transform (in 2-D) prior to a 1-D wavelet transform (Boukerbout, 2004; Boukerbout and Gibert, 2006; Sailhac et al., 2009). More than localization, this method leads to an image of the anomalies causative structures both in the 2-D and 3-D cases.

In the present study, we use the complex ridgelet transform since we use complex analyzing wavelets (Sailhac et al., 2000; Boukerbout et al., 2003). The imaginary part of the latter is the Hilbert transform of their real part, thus the wavelets are analytic signals whose

ACCEPTED MANUSCRIPT

envelop (or modulus) and phase can be computed. The inclination of identified sources is obtained from the phase of the complex continuous transform (Sailhac et al., 2000). Both the modulus and the phase of the ridgelet transform display conspicuous cone-like patterns associated with each analyzed anomaly (Boukerbout and Gibert, 2006). The cone-like appearance apex is pointing onto the source depth and its likelihood is practically evaluated with entropy criteria (Tass et al., 1998; Boukerbout et al., 2003; Boukerbout and Gibert, 2006).

The results obtained from the aeromagnetic data analysis in the case 3-D, are shown in figure 6. The structures responsible of magnetic anomalies are shown in the top of figure while their location in the crust is shown in bottom. The 3-D image of the Chlef region is complex as well as its geological context and seismotectonic sketch.

Figure 6.

The identified structures consist of a juxtaposition of prismatic bodies or blocks at various depths along the range of observed depths.

The deepest structures identified from aeromagnetic data are elongated in E-W direction and are bordering the region in its northern and southern parts. Their depth reaches 31 km within the offshore magnetic anomaly; 20 km along the coast within volcanic structures and 29 km in the South within Ouarsenis Mounts. The general tendencies of the identified structures in the Chlef basin are NE-SW, NW-SE and E-W, with a depth ranging from near surface to 25 km. The N-S structures within the Chlef basin are located between depths varying from 9 to 16 km. In the North (offshore), the N-S structures limiting westward coastal and offshore anomalies reach 20 km of depth.

The present deformation in the Chlef basin is mainly related to a transpression with N-S to NNW-SSE shortening direction, which is expressed by active tectonic responsible of the earthquake activity (Philippe & Meghraoui, 1983, Meghraoui et al., 1986; Meghraoui and

ACCEPTED MANUSCRIPT

Pondrelli, 2012; Medaouri et al., 2014). The NE-SW trending folds and NE-SW active sinistral transpressive faults were activated during the 1954 and 1980 destructive earthquakes (Bezzeghoud et al., 1995; Ouyed et al., 1981). These reverse faults and related folding are disposed on right lateral echelon and should be coupled with NW-SE to E-W trending strike-slip deep active faults (Meghraoui, 1982, 1986, 1988; Thomas, 1985; Chiarabba et al, 1997). The NE-SW faults are associated with asymmetric folds and the different tectonic structures define some NE-SW blocks (Thomas, 1985; Morel & Meghraoui, 1996). A kinematics model of block rotation related to a transpression with NNW-SSE direction of plates convergence, is proposed in the Chlef basin (Meghraoui et al., 1996) where the blocks rotation was previously studied with paleomagnetic investigations by Aïfa et al., 1992 and recently by (Derder et al., 2011; Derder et al., 2013; Aifa, 2014).

Figure 7.

The compilation of all these identified magnetized features from different analyzing methods is reported on the shaded map and correlated with the seismicity of the area (Figure 7). Many of identified structures are located on active zones. The recognized lineaments show polygonal shapes at different scales and corroborate the theory of structure in blocks of the Chlef basin as defined by many authors.

We would like to sketch out the shape of the topography of the magnetized substratum and how are connected the identified structures in depth. So we choose to process an N-S profile running across the magnetic anomalies from the Mediterranean Sea until Ouarsenis mounts, throughout the sedimentary basin in the Oued Fodda area. This profile extracted from the magnetic anomaly map, is located at longitude of 1°40'E. We use the complex one dimensional wavelet transform (Sailhac et al., 2000; Boukerbout et al., 2003) to analyze it. The modulus and the phase values of the complex wavelet coefficients allow us to identify both the depth and the dip of the structures.

ACCEPTED MANUSCRIPT

Figures 8a, 8b, 8c, 8d, 8e.

The figure "8 a" represents the corresponding topographic and bathymetric profile. The altitudes in this area vary from 500 to 1500m onshore and reach -2700m offshore. This suggests that the area is very steep.

The N-S structural cross-section (figure 8 b) along the profile shows that the area displays in surface folds and thrusting accidents, trending from NE-SW to ENE-WSW directions. The folds result from transpressive phases related to thrusting accidents. In subsurface the basin is affected by sub-vertical accidents. The substratum (African and Maghrebides) outcrop in the North and is rising in the basin.

The intensity of the magnetic anomaly (Figure 8 c Top) varies from -40 to +40nT.

The modulus of the continuous wavelet transform (Figure 8 c Middle) shows the signature of many contacts or faults. The depth of the identified magnetized structures along this profile, using the maximum entropy criteria (Figure 8 c Bottom), is ranging between 6 and 30km. The very deep magnetized structures are located mainly in the Ouarsenis Mounts area and in the Mediterranean Sea, while the less deep ones are located in the sedimentary basin and give an estimation of its thickness. From South to North along the profile, in the Ouarsenis Mounts area, the first identified fault is located at the latitude of 3975km and at depth of 8 km. The phase of the wavelet transform (Figure 8 d) identifies this fault with an inclination of 90°. The second fault is located at latitude of 3996km and at depth of 14km with an inclination of 90°. The third fault identified in this area is located at latitude of 4002 km at depth of 10km with an inclination of 50°. In the Oued Fodda- El Abadia region, the first fault is identified at latitude of 4010km (O. Fodda) at depth of 6km with an inclination of 30°, this is confirmed by the results of dislocation model of vertical movements for this area (Bezzeghoud et al., 1995). The second fault is located at latitude of 4020km at depth of 14km with an inclination of 54°. In the Bou Maâd-Damous area, the identified magnetized

ACCEPTED MANUSCRIPT

substratum is located at latitudes between 4030km (Bou Maâd) and 4047 km (Damous) and depth ranging from 20km to 29km (Volcanism of Damous) with an inclination varying from 90° to 160°. The last part of this profile is over the Mediterranean Sea. Here we depict three contacts or faults located at latitudes of 4050, 4056 and 4066km and at depth of 16, 18 and 24km and inclination of 180°, 170° and 100° respectively. The first idea without any assumption we have, in modeling this part of the profile, is that, the deep structure offshore is a basaltic structure where, some mantle material more susceptible than basalt, intrudes through the contacts and faults. The second interpretation for this offshore part of profile according to the identified structures and different studies in the Mediterranean Sea (Galdeano and Rossignol, 1977; Mauffret et al., 1987; Gelabert et al., 2002; Mauffret et al., 2004; Cavazza et al., 2004; Domzig et al., 2006; Leprêtre et al., 2013; Badji et al., 2014; Bouyahiaoui et al., 2015), that the identified structures may correspond to the boundary between two blocks with different susceptibilities, and could be the limit of African and Eurasian plates in the Miocene, when the opening of the Mediterranean Sea happened and the AlKaPeCa blocks were drifted and collided with the African plate.

Along this profile, some deep identified structures are well correlated with the seismicity along the profile and the observed structures on the structural cross-section (Figure 8 e), either by merging, extending those in the same direction or shifting those in the perpendicular one. Whereas many others complete the structural information. There is also a good correlation with other geophysical and geological studies (Ouyed et al., 1983; Meghraoui, 1988; Avouac et al., 1992; Bezzeghoud et al., 1995; Aifa et al., 2003; Yelles et al., 2006; Afalfiz et al., 2009; Beldjoudi et al., 2012; Abtout et al., 2014).

ACCEPTED MANUSCRIPT

7. Correlation between magnetic and gravity results

We compare the results obtained from magnetic data analysis with those obtained with the gravity ones (Abtout et al., 2014), especially in the Chlef basin, where there is a good gravity data curvature.

The common anomalies observed both on the gravimetric and magnetic maps correlated to geological data, correspond, in the West part of the studied area, to bodies within the Chlef basin. The Boukadir positive magnetic anomaly, which is negative in gravity, is made up of two lobes disrupted by a discontinuity in the NW-SE direction. In a northward, there is a negative magnetic anomaly corresponding to the Ouled Fares anticline and appears also negative on the gravity map. The positive anomaly in the East is identified on the Doui massif, which is better defined, but appears very weak on the gravity map. The negative one coincides with the positive gravimetric anomaly and is located upon the thrusting Jurassic massifs of Temoulga and Rouina.

Many discontinuities are identified (Figure 7). The NW-SE discontinuity is thrusting in the sinistral way the Boukadir anomaly. It corresponds to the gravimetric discontinuity which limits the basin with the uplifted substratum. The next one is perpendicular to the first and is identified in the South of the Boukadir anomaly. It coincides with Relizane Fault observed on the gravity map. More in the North of this discontinuity, two discontinuities appear and may correspond to El Asnam and Relizane Faults. In the East, between the negative magnetic anomaly and the positive one appears a discontinuity which may be correspond to the Palaeozoic substratum known in the South. All identified common features appear deeper from the magnetic data analysis, especially E-W structures bordering the north and south limits of the basin.

ACCEPTED MANUSCRIPT

8. Conclusion

The aeromagnetic map of the Chlef region shows good correlation with the known geological features and structures. Furthermore, the aeromagnetic map reveals magnetized bodies that are not easily recognized in the field because buried or unreachable as those identified in the Mediterranean Sea. The aeromagnetic map thus contributes to the geological interpretation onshore and offshore. The information obtained from magnetic data is complementary or identical to gravimetric and geological ones and converges to the same interpretation.

The aeromagnetic maps show some positive short wavelength anomalies along the coast, corresponding to the calc-alkaline volcano formations. While in the North in Mediterranean Sea, in the West and in the South of the studied area, appear the positive long wavelength anomalies. The structures responsible of these anomalies are very deep-rooted. The negative anomalies in the basin are associated to the deep Palaeozoic substratum. The upward continued maps at different altitudes suggest that the thickness of the basin is not uniform and is at a meaning value of 5 km. Moreover, it confirms the uplift of the basin in its southern part. The identification of the magnetized material, show that the most deepest structures bounding the basin in the North and in the South, are oriented in the E-W direction and reaches the 31 km of deep. Many discontinuities are identified; those very deep affecting the Palaeozoic substratum, in addition to the known faults as the Oued Fodda, Boukadir and Relizane ones. The particular positive magnetic anomaly of Boukadir, in the Chlef basin may correspond to a succession of basaltic sills embedded between calcareous formations and which may be occurred in the Tortonian extension phase as suggested by many authors. The

ACCEPTED MANUSCRIPT

compilation of all identified magnetic features on the shaded anomaly map shows geometric shape which corroborates the theory of the structure in blocks of the Chlef area.

Acknowledgements

This work was supported by CMEP Project 08MDU752. We are grateful to A. Yelles, H. Djellit, A. Boudiaf, F. Aït Hamou, D. Belhaï, A. Afalfiz and S. Maouche for different discussions. We especially thank Pr. Li Zhen Cheng for his useful suggestions. We also thank the editor and the reviewers for their constructive remarks and comments.

References

Abtout A., Boukerbout, H., Gibert, D., 2014. Gravimetric evidences of active faults and underground structure of the Chlef seismogenic basin (Algeria). J. Afr. Earth Sci., http://dx.doi.org/10.1016/j.jafrearsci.2014.02.011

Afalfiz A., Belhaï, D., Djemaï, N., 2009. Mise en évidence d'une minéralisation à Ba ± (Cu, Fe, Ni) à la limite (Zones internes/Zones externes) des Maghrébides, dans la région de Béni Aquil (Béni Haoua, Ouest Tipaza, Algérie). 7ème Journées des Sciences de la Terre. FSTAGT/USTHB. Alger.

Aïfa, T., 2014. Neogene rotations of the Chenoua massif, northern Algeria, from remagnetizations. Arab J. Geosci. DOI 10.1007/s12517-013-1124-x.

Aïfa T., Zaagane, M., 2014. Neotectonic deformation stages in the central Ouarsenis culminating zone, Northwestern Algeria. Arab J. Geosci. DOI 10.1007/s12517-014-1385-z.

Aïfa, T., Feinberg, H., Derder, M.E.M., Merabet, N., 2003. Contraintes magnétostratigraphiques concernant la durée de l'interruption des communications marines en Méditerranée occidentale pendant le Messinien supérieur. Geodiversitas 25(4) : 617-631.

ACCEPTED MANUSCRIPT

Aïfa T, Feinberg H, Derder MEM, Merabet N (1992) Rotations paléomagnétiques récentes dans le bassin du Chéliff (Algérie). C R Acad Sci Paris 314:915–922

Aït Hamou, F., 1987. Etude pétrologique et géochimique du volcanisme d'âge Miocène de la région de Hadjout (Ouest algérois). Thèse de Magister, USTHB, Alger (Algérie).

Alexandrescu, M., Gibert, D., Hulot, G., Le Moüel, J. L. and Saracco, G., 1995. Detection of geomagnetic jerks using wavelet analysis. J. Geophys. Res. 100, 12,557-12,572.

Alexandrescu, M., Gibert, D., Hulot, G., Le Moüel, J. L. and Saracco, G., 1996. Worldwide wavelet analysis of geomagnetic jerks. J. Geophys. Res. 101, 21,975-21,994.

Anderson, H., Jackson, J., 1987. Active tectonics of the Adriatic region. Geophys. J. R. astr. Soc., 91, 937-983.

Anderson, R.V., 1936. Geology in the coastal atlas of western Algeria. Memoir Geological Society of America, 4, 450 p.

Avouac, J.P., Meyer, B., Tapponier, P., 1992. On the growth of normal faults and the existence of flats and ramps along the El Asnam active fold and thrust system. Tectonics, 11(1):1-11.

Badji, R., Charvis, P., Bracene, R., Galve, A., Badsi, M., Ribodetti, A., Benaissa, Z., Klingelhoefer, F., Medaouri, M., Beslier, M.O., 2015. Geophysical evidence for a transform margin offshore Western Algeria: a witness of a subduction-transform edge propagator?. Geophys. J. Int., 200, 1029-1045.

Beldjoudi, H., Delouis, B., Heddar, A., Nouar, O., B., Yelles-Chaouche, A., 2012. The Tadjena Earthquake (Mw=5.0) of December 16, 2006 in the Chlef Region (Northern Algeria): Waveform Modeling, Regional Stress, and Relation with the Boukadir Fault. Pure Appl. Geophys. 169 (2012), 677-691. DOI 10.1007/s00024-011-0337-8.

ACCEPTED MANUSCRIPT

Bellon, H., Guardia, P., 1980. Le volcanisme alcalin plio-quaternaire d'Algérie occidentale. Etude radiométrique et paléomagnétique. Rev. Géogr. Phys. Géol. dyn., 22, (3), 213-222.

Bezzeghoud, M., Dimitrov, D., Ruegg, J. C., Lammali, K., 1995. Faulting mechanism of the El Asnam (Algeria) 1954 and 1980 earthquakes from modelling of vertical movements. Tectonophysics, 249, 249-266.

Boschetti, F., Hornby, P., Horowitz, F., G., 2001. Wavelet based inversion of gravity data. Exploration Geophysics. 32 (1), 48-55.

Boschetti, F., Therond, V., Hornby, P., 2004. Feature removal and isolation in potential field data, Geophys. J. Int., 159, 833-841, doi:10.1111/j1365-246X.2004.02293.x.

Boukerbout, H., Abtout, A., 2000. Identification of Western Algeria faults using aeromagnetic data. International symposium: « Dynamic Evolution of Active Faulting in the Mediterranean Region » Algiers, Algeria, October 2000.

Boukerbout, H., Gibert, D., Sailhac, P., 2003. Identification of sources of potential fields with the continuous wavelet transform: Application to VLF data, Geophys. Res. Lett., 30(8), 1427, doi: 10.1029/2003GL016884.

Boukerbout, H., Gibert, D., 2006. Identification of sources of potential fields with the continuous wavelet transform: Two-dimensional ridgelet analysis. Journal of Geophysical Research, Vol. 111, B07104, doi: 10.1029/2005JB004078.

Boukerbout, H., Abtout, A., 2010. Le champ aéromagnétique algérien: champ magnétique total ou champ d'anomalie ? Bulletin du Service Géologique National. Vol. 21, n° 2, pp. 183-200.

Bousquet, J. C., Philip, H., 1981. Les caractéristiques de la Néotectonique en Méditerranée occidentale. In Sedimentary basins of the Mediterranean margins, edited by C. F. Wezel, Tecnoprint, Bologna, 389-405.

ACCEPTED MANUSCRIPT

Bouyahiaoui, B., Sage, F., Abtout, A., Klingelhoefer, F., Yelles-Chaouche, K., Schnürle, P., Marok, A., Dévèrchere, J., Arab, M., Galve, A. and Collot, J. Y., 2015. Crustal structure of the eastern Algerian continental margin and adjacent deep basin: implications for late Cenozoic geodynamic evolution of the western Mediterranean. Geophys. J. Int.201, 1912-1938.

Bufforn, E., San de Galdeano C., Udias A., 1995. Seismotectonics of the Ibero-Maghrebian region. Tectonophysics, 248, 247-261.

Candès, M., 1998. Ridgelets: Theory and Applications, Ph.D. thesis, Dep. Of Stat., Stanford Univ., Stanford, Calif.

Candès, M., Donoho, D. L., 1999. Ridgelets : A key to higher-dimensional intermittency ? Philos. Trans. R. Soc. Ser. A, 357, 2495-2509.

Cavazza, W., Roure, F.M., Spakman, W., Stampfli, G.M., Ziegler, P.A., 2004. The Transmed Atlas – The Mediterranean Region from Crust to Mantle. Springer, Berlin, Heidelberg.

Chamoli, A., Pandey, A. K., Dimri, V. P. and Banerjee, P., 2011. Crustal configuration of the Northwest Himalaya based on modeling of gravity data. Pure Appl. Geophys., 168, 827-844, doi:10.1007/s00024-010-0149-2.

Chiarabba, C., Amato, A. & Meghraoui, M. (1997). Tomographic images of the El Asnam fault zone and the evolution of a seismogenic thrust-related fold. Journal of geophysical Research., 102(B11), 24,485–24,498, doi:10.1029/97JB01778

Cooper, G. R. J., 2006. Interpreting potential field data using continuous wavelet transforms of their horizontal derivatives. Computers & Geosciences, 32, 984-992, doi:10.1016/j.cageo.2005.10.012

ACCEPTED MANUSCRIPT

Delteil, J., 1974. Tectonique de la chaîne alpine en Algérie d'après l'étude du Tell oranais oriental : Monts de la Mina, Beni-Chougrane, Dahra. Thèse des Sci. Université de Nice, France.

Derder, M.E.M., Henry, B., Amenna, M., Bayou, B., Maouche, S., Besse, J., Abtout, A., Boukerbout, H., Bessedik, M., Bourouis, S., Ayache, M., 2011. Tectonic evolution of the active 'Chelif' Basin (Northern Algeria) from paleomagnetic and magnetic fabric investigations. New Frontiers in Tectonic Research at the Midst of Plate Convergence. Intech Publisher book. Intech Publisher. ISBN: 978-953-307-594-5, pp. 3–26.

Derder, M.EM., Henry, B., Maouche, S., Bayou, B., Amenna, M., Besse, J., Bessedik, M., Belhai, D., Ayache, M., 2013. Transpressive tectonics along a major E-W crustal structure on the Algerian continental margin: Blocks rotations revealed by a paleomagnetic analysis. Tectonophysics 593, 183-192.

Dewey, J.F., Helman, M.L., Turco, E., Hutton, D.H.W., Knott, S.D., 1989. Kinematics of the western Mediterranean. In: Coward, M.P., Dietrich, D., Park, R.G. (Eds.), Alpine Tectonics. Geological Society, London, pp. 265–283.

Dewey, J.W., 1991. The 1954 and the 1980 Algerian earthquakes :implications for the characteristic-displacement model of fault behavior. Bulletin of the Seismological Society of America, Vol. 81, No. 2, pp. 446-467.

Domzig, A., Yelles, A.K., Le Roy, C., Déverchère, J., Bouillin, J.P., Bracène, R., Mercier de Lépinay, B., Le Roy, P., Calais, E., Kherroubi, A., Gaullier, V., Savoye, B., Pauc, H., 2006. Searching for the Africa–Eurasia Miocene boundary offshore western Algeria (MARADJA'03 cruise). C. R. Geoscience 338, 80–91

Fedi, M. and Quarta, T., 1998. Wavelet analysis for the regional-residual and local separation of potential field anomalies. Geophysical Prospecting 46, 507-525.

ACCEPTED MANUSCRIPT

Fedi, M., Premiceri, R., Quarta, T., Villani, A. V., 2004. Joint application of continuous and discrete wavelet transform on gravity data to identify shallow and deep sources. Geophys. J. Int., 156, 7-21, doi:10.1111/j1365-246X.2004.02118.x.

Fedi, M., Cella, F., Quarta, T., Villani, A. V., 2010. 2D Continuous wavelet transform of potential fields due to extended source distributions. Appl. Comput. Harmon. Anal. 28, 320-337. doi :10.1016/j.acha.2010.03.002.

Fedi, M., and Cascone, L., 2011. Composite continuous wavelet transform of potential fields with different choices of analyzing wavelets. J. Geophys. Res., 116, B07104, doi :10.1029/2010JB007882.

Galdeano, A., Rossignol, J.-C., 1977. Assemblage à altitude constant de cartes d'anomalies magnétiques couvrant l'ensemble du bassin occidental de la Méditerranée. Bull. Soc. Géol. France. 7, 461-468.

Gelabert, B., Sabat, F., Rodriguez-Perea, A., 2002. A new proposal for the Late Cenozoic geodynamic evolution of the western Mediterranean. Terra Nova 14, 93-100.

Gibert, D., Pessel, M., 2001. Identification of sources of potential fields with the continuous wavelet transform: Application to self-potential profiles, Geophys. Res. Lett., 28 1863-1866.

Gibert, D., and Sailhac, P., 2008. Comment on ‘‘Self-potential signals associated with preferential groundwater flow pathways in sinkholes’’ by A. Jardani, J. P. Dupont, and A. Revil, J. Geophys. Res., 113, B03210, doi:10.1029/2007JB004969.

Girardin, N., Hatzfeld, D., Guiraud, R., 1977. La séismicité du Nord de l'Algérie. C.R. somm. Soc. Géol. Fr., 2, 95-100.

Girod, M., Girod, N., 1977. Contribution de la pétrologie à la connaissance de l'évolution de la Méditerranée occidentale depuis l'Oligocène. Bull. Soc. Géol. France. 7, XIX, (3), 481-488.

ACCEPTED MANUSCRIPT

Goupillaud, P., Grossmann, A., Morlet, J., 1984. Cycle-octave and related transforms in seismic signal analysis, Geoexploration, 23, 85-102.

Grossmann, A. and Morlet, J., 1984. Decomposition of Hardy functions into square integrable wavelets of constant shape. SIAM J. Math. Anal., 15, 732-736.

Grossmann, A., Holschneider, M., Kronland-Martinet, R., and Morlet, J., 1987. Detection of abrupt changes in sound signals with the help of wavelet transforms. Advances in Electronics and Electron Physics, vol. 19, pp. 289-306, Elsevier, New York.

Groupe de Recherche néotectonique de l'arc de Gibraltar, 1977. L'histoire tectonique récente (Tortonien à Quaternaire) de l'Arc de Gibraltar et des bordures de la mer d'Alboran. Bull. Soc. Géol. France, XIX, 3, 575-614.

Hernandez, J., Lepvrier, C., 1976. Pétrographie des laves liées aux bassins de l'Ouest algérois. Comparaison avec le volcanisme du Rif et de l'Oranais. Réunion Ann. Sci. Terre, Paris, 4, 222.

Holschneider, M., 1988. On the wavelet transformation of fractal objects. J. Stat. Phys., 50, 953-993.

Holschneider, M., 1995. Wavelets: An Analysis Tool. 423 pp., Clarendon, Oxford, U.K.

Hornby, P., Boschetti, F., Horovitz, F.G., 1999. Analysis of potential field data in the wavelet domain, Geophys. J. Int., 137, 175-196.

Idres, M., Ydri, A., Lefort, J.P., Aïfa, T., 1996. Proposition d'un schéma structural du bassin du Chélif (Algérie) à partir des données gravimétriques. C.R. Aca. Sci. Paris. 322, IIa, 322, 85-91.

Idres, M., Lefort, J.P., Aïfa, T., 1998. Modélisations gravimétriques et magnétiques des structures profondes du bassin du Chélif (Algérie). Bulletin du Service Géologique de l'Algéri, 9, 1, 21-32.

ACCEPTED MANUSCRIPT

Karnik, V., 1969. Seismicity of the European Area, Vol. 1. Dordrecht, Holland: D. Reidel. 364 pp.

King, G. C. P., Vita Finzi, C., 1981. Active folding in the Algerian earthquake of 10 October 1980, Nature, 292, 22-26.

Kireche, O., 1977. Etude géologique structurale des massifs de la plaine du Chélif (Doui, Rouina, Temoulga). Thèse Doct. 3è cycle, USTHB, Alger (Algérie).

Lammali, K., Bezzeghoud, M., Oussadou, F., Dimitrov, D., Benhallou, H., 1997. Postseismic deformation at El Asnam (Algeria) in the seismotectonic context of north-western Algeria. Geophys. J. Int., 129, 597-612.

Leblanc G., E., and Morris, W., A., 2001. Denoising of aeromagnetic data via the wavelet transform. Geophysics, 66, 1793-1804.

Le Pichon, X., Bergerat, F., Roulet, M.J., 1988. Plate kinematics and tectonic leading to Alpine belt formation: a new analysis, processes in continental lithospheric deformation. Geological Society of America Special Paper 111–131.

Leprêtre, A., Klingelhoefer, F., Graindorge, D., Schnurle, P., Beslier, M. O., Yelles, K., Déverchère, J. & Bracene, R., 2013. Multiphased tectonic evolution of the Central Algerian margin from combined wide-angle and reflection seismic data off Tipaza, Algeria. J. Geophys. Res.: Solid Earth, 118, 1-18.

Li, Y., and Oldenburg, D., W., 2003. Fast inversion of large-scale magnetic data using wavelet transforms and a logarithmic barrier method. Geophysical Journal International. 152, 251-265.

Mallat, S., and Hwang, W. L., 1992. Singularity detection and processing with wavelets. IEEE Trans. Inf. Theory. 38, 617-643.

ACCEPTED MANUSCRIPT

Martelet, G., Sailhac, P., Moreau, F., Diament, M., 2001. Characterization of geological boundaries using 1-D wavelet transform on gravity data: Theory and application to the Himalayas. Geophysics, 66, 1116–1129.

Mattauer, M., 1958. Etude géologique de l'Ouarsenis oriental, Algérie. Publ. Serv. Carte Géol. Algérie, 758.

Mauffret, A., El Robrini, M., Gennesseaux, M., 1987. Indice de la compression récente en mer Méditerranée : un bassin losangique sur la marge nord-algérienne. Bull. Soc. Géol. France 8, 1195-1206.

Mauffret A., Frizon de Lamotte, D., Lallemant, S., Gorini, C., Maillard, A., 2004. E-W opening of the Algerian Basin (Western Mediterranean). Terra Nova 16, 257-264.

Mauri, G., Williams-Jones, G., Saracco, G., 2010. Depth determinations of shallow hydrothermal systems by self-potential and multi-scale wavelet tomography. J. Volcanol. Geotherm. Res., doi:10.1016/j.jvolgeores.2010.02.004

Maury, R.C., Fourcade, S., Coulon, C., El Azzouzi, M., Bellon, H., Coutelle, A., Ouabadi, A., Semroud, B., Megartsi, M., Cotten, J., Belanteur, O., Louni, A., Piqué, A., Capdevila, R., Hernandez, J., Réhault, J.P., 2000. Post-collisional Neogene magmatism of the Mediterranean Maghreb margin: a consequence of slab breakoff. Earth and Planetary Sciences, 331, 159-173.

Mazzoli, S., Helman,M., 1994.Neogene patterns of relative platemotion for Africa–Europe: some implications for recent central Mediterranean tectonics. Geologische Rundschau 83, 464–468.

McDonald, A.J.W., Fletcher, C.J.N., Carruthers, R.M., Wilson, D., Evans R.B., 1992. Interpretation of the regional gravity and magnetic surveys of Wales, using shaded relief and Euler deconvolution techniques. Geol. Mag. **129** (5), pp. 523-531.

ACCEPTED MANUSCRIPT

Medaouri, M., Devérechère, J., Graindorge, D., Bracene, R., Badji, R., Ouabadi, A., Yelles, K. & Bendib, F., 2014. The transition from Alboran to Algerian basins (Western Mediterranean Sea): chronostratigraphy, deep crustal structure and tectonic evolution at the rear of a narrow slab rollback system. J. Geodyn., 77, 186-205.

Meghraoui, M., 1982. Etude néotectonique de la région Nord-Ouest d'El Asnam : Relation avec le séisme du 10 octobre 1980. Thèse Doct. 3ème cycle, Université de Paris VII, France.

Meghraoui, M., Cisternas, A., Philip, H., 1986. Seismotectonics of the lower Chelif basin: structural background of the El Asnam (Algeria) earthquake. Tectonics, 5, 6, 809-836.

Meghraoui, M., 1988. Géologie des zones sismiques du nord de l'Algérie (paléosismicité, tectonique active et synthèse sismotectonique). Thèse Doct. Es. Sci., Université de Paris Sud, France.

Meghraoui, M., Morel, J.L., Andrieux, J., Dahmani, M., 1996. Tectonique plio-quaternaire de la chaîne tello-rifaine et de la mer d'Alboran. Une zone complexe de convergence continent-continent. Bull. Soc. Géol. France. 167, 1, 141-157.

Meghraoui, M., Pondrelli, S., 2012. Active faulting and transpression tectonics along the plate boundary in North Africa. Annals of Geophysics 55 (5), 2012. http://dx.doi.org/10.4401/ag-4970.

Minster, J.B., Jordan, J.H., 1978. Present-day plate motions. J. Geophys. Res., 83, 5331-5354.

Moreau, F., Gibert, D., Holschneider, M., Saracco, G., 1997. Wavelet analysis of potential fields, Inverse Probl., 13, 165-178.

Moreau, F., Gibert, D., Holschneider, M., Saracco, G., 1999. Identification of sources of potential fields with the continuous wavelet transform: Basic theory, J. Geophys. Res., 104, 5003-5013.

ACCEPTED MANUSCRIPT

Morel, J.L. & Meghraoui, M., 1996. Goringe-Alboran-Tell tectonic zone; a transpression system along the Africa-Eurasia plate boundary. Geology, 1996, 24, 8, 755-758.

Ouyed, M., 1981. Le tremblement de terre d'El Asnam du 10 octobre 1980. Etude des répliques. Thèse 3ème cycle, Université Scientifique et Médicale de Grenoble, France.

Ouyed, M., Meghraoui, M., Cisternas, A., Deschamps, A., Dorel, J., Frechet, J., Gaulon, R., Hatzfeld, D., Philip, H., 1981. Seismotectonics of the El Asnam earthquake. Nature, 292, 5818, 26-31.

Ouyed, M., Yielding, G., Hatzfeld, D., King, G.C.P., 1983. An aftershock study of the El Asnam (Algeria) earthquake. Geophys. J. R. Astr. Soc., 73, 605-639.

Paterson, Grant and Watson Limited, 1976. Réinterprétation des levés aéromagnéto-spectrométriques de l'Algérie. 3 volumes, rapport interne ORGM.

Perrodon, A., 1957. Etude géologique des basins néogènes sub-littoraux de l'Algérie nord occidentale. Bull. Serv. Carte Géol. Algérie, 12, 343.

Philip, H., Thomas, G., 1977. Détermination de la direction de raccourcissement de la phase de compression quaternaire en Oranie (Algérie). Rev. Géogr. Phys. Géol. dyn., 19, (4), 315-324.

Philip, H., Meghraoui, M., 1983. Structural analysis and interpretation of the surface deformations of the El Asnam earthquake of October 10, 1980. Tectonics, 2, 1, 17-49.

Pouliquen, G., and Sailhac, P., 2003. Wavelet analysis of deep-two magnetic profiles: Modeling the magnetic layer thickness over oceanic ridges. Journal of Geophysical Research 108, 2297-2315.

Ricou, L.E., 1994. Tethys reconstructed: plates continental fragments and their boundaries since 260 Ma from Central America to South-eastern Asia. Geodinamica Acta 7 (4), 169–218.

ACCEPTED MANUSCRIPT

Ridsdill-Smith, T. A., and Dentith, M. C., 1999. The wavelet transform in aeromagnetic processing. Geophysics, 64, 1003-1013.

Rosenbaum, G., Lister, G.S., Duboz, C., 2002. Relative motions of Africa, Iberia and Europe during Alpine orogeny. Tectonophysics 359 (1–2), 117–129.

Rothé, J.P., 1950. Les séismes de Kherrata et la séismicité en Algérie. Pub. Serv. Carte Géol. Algérie, 24.

Sailhac, P., Galdeano, A., Gibert, D., Moreau, F., Delor, C., 2000. Identification of sources of potential fields with the continuous wavelet transform: Complex wavelets and application to aeromagnetic profiles in French Guiana. J. Geophys. Research, 105, 19455–19475.

Sailhac, P., Marquis, G., 2001. Analytic potentials for the forward and inverse modelling of SP anomalies caused by subsurface fluid flow, Geophys. Res. Lett., 28,1851-1854.

Sailhac, P., Gibert, D., 2003. Identification of sources of potential fields with the continuous wavelet transform: Two-Dimensional wavelets and multipolar approximation, J. Geophys. Res., 108(B5), 2262, doi: 10.1029/2002JB002021.

Sailhac, P., Gibert, D., Boukerbout, H., 2009. The theory of the continuous wavelet transform in the interpretation of potential fields: a review. Geophysical Prospecting, Vol. 57, No. 4. pp. 517-525.

Saracco, G., Labazuy, P., and Moreau, F., 2004. Localization of self-potential sources in volcano-electric effect with complex wavelet transform and electrical tomography methods for an active volcano. Geophys. Res. Lett., 31, L12610, doi: 10.1029/2004GL019554.

Schettino, A., Turco, E., 2006. Plate kinematics of the Western Mediterranean region during the Oligocene and Early Miocene. Geophys. J. Int. 1-26, http://dx.doi.org/10.1111/j.1365-246X, 2006.02997.x.

ACCEPTED MANUSCRIPT

Tapponier, P., 1977. Evolution tectonique du système alpin en Méditerranée ; poinçonnement et écrasement rigide plastique. Bull. Soc. Géol. France, 19, 437-460.

Tass, P., Rosemblum, M. G., Weule, J., Kurths, J., Pikovsky, A., Volkmann, J., Schnitzler, A.,Freund, H.-J., 1998. Detection of n:m phase locking from noisy data: application to magneto encephalography. Phys. Rev. Lett., 81, 3291-3294.

Trad, D. O., and Travassos, J. M., 2000. Wavelet filtering of magnetotelluric data. Geophysics, Vol. 65, N° 2, p. 482-491.

Thomas, G., 1974. La phase de compression Pléistocène en Algérie nord occidentale : âge, premiers éléments cinématiques, relation avec les mouvements en distension. C.R. Acad. Sci., 279, 311-314.

Thomas, G., 1985. Géodynamique d'un bassin intra montagneux : le bassin du Bas Chlef occidental (Algérie) durant le Moi-Plio-Quaternaire. Thèse Doctorat, Université de Pau, France.

Vallée, M. A., Keating, P., Smith, R. S., and St-Hilare, C., 2004. Estimating depth and model type using the continuous wavelet transform of magnetic data. Geophysics, 69, 191-199.

Yang, Y. S., Li, Y. Y., Liu, T. Y., 2010. Continuous wavelet transform, theoretical aspects and application to aeromagnetic data at the Huanghua Depression, Dagang Oilfield, China. Geophysical Prospecting. 58, 669-684.

Yelles, A.K., Boudiaf, A., Djellit, H., Bracène, R., 2006. La tectonique active de la région nord-algérienne. C. R. Géosciences. 338, 126-139.

Yelles, A., Domzig, A., Déverchère, J., Bracene, R., Mercier de Lépinay, B., Strzerzynski, P., Bertrand, G., Boudiaf, A., Winter, T., Kherroubi, A., Le Roy, P., Djellit, H., 2009. Plio-quaternary reactivation of the Neogene margin off NW Algiers, Algeria: The Khayr al Din bank. Tectonophysics, 475(1), 98-116.

ACCEPTED MANUSCRIPT

Ydri, A., 1988. Etude gravimétrique de la région d'Ech-Chlef. Thèse Magister, USTHB, Alger, Algérie.

Yielding, G., Ouyed, M., King, G.C.P., Hatzfeld, D., 1989. Active tectonics of the Algerian Atlas Mountains – eviden ce from aftershocks of the 1980 El Asnam earthquake. Geophys. J. Int. 99, 761-788.

List of figures

Figure 1. Geological map of the Chlef region (Modified from Meghraoui et al., 1986). The studied area (four-sided figure) is located in a box ranging from: 00°33'- 02°00'E in longitude and 35°48'-36°56'N in latitude.

Figure 2. Aeromagnetic map of Chlef region: total field anomaly reduced to the pole.

Figure 3. Aeromagnetic map of Chlef region: total field anomaly 5 km upward continued for showing long wavelengths.

Figure 4. Aeromagnetic map of Chlef region: shaded map of total field anomaly reduced to the pole. This map allows seeing the magnetized structures and the correspondence with geological features.

Figure 5. Aeromagnetic map of Chlef region: vertical gradient of the total field anomaly. Many magnetic lineaments appear corresponding to known and unknown geological contacts.

Figure 6. 3-D imaging of magnetized structures identified from the wavelet and ridgelet transforms (top) and their locations in the crust (bottom). The North direction is given by the latitude axis. The colour scale corresponds to the maximum entropy criteria (Tass et al., 1998; Boukerbout et al., 2003; Boukerbout and Gibert, 2006; Sailhac et al., 2009) for selecting sources location.

ACCEPTED MANUSCRIPT

Figure 7. The compilation of identified magnetized features (black lines) from different analyzing methods reported on the shaded map and correlation with seismicity of the area (small, intermediate and big circles: 2<M<3, 3<M<4 and M>4).

Figure 8 a. The topographic and bathymetric profile along the N-S aeromagnetic profile. The altitudes in this area vary from 500 to 1500m onshore and reach -2700m offshore.

Figure 8 b. Structural cross-section along the N-S profile (Dahra-Bou Maad, Chlef basin, Ouarsenis Mountains) outlining folds and accidents (Modified from Megartsi, 1996).

Figure 8 c. Identification of the magnetized substratum along the N-S profile using the modulus of continuous wavelet transform. The intensity of the magnetic anomaly (top) varies from -45 to +40nT.

The modulus of the continuous wavelet transform (middle) shows the signature of many contacts or faults. The depth (bottom) of the identified magnetized structures along this profile using the maximum entropy criteria is ranging between 6 and 30km. The deepest magnetized structures are located in the Ouarsenis Mounts (in the South) area and along the coast and in the Mediterranean Sea (in the North).

Figure 8 d. The phase of the wavelet transform gives the inclination of the identified contacts.

Figure 8 e. Correlation between identified structures with the continuous wavelet transform, the seismicity along the profile and the structural cross-section.

ACCEPTED MANUSCRIPT

ACCEPTED MANUSCRIPT

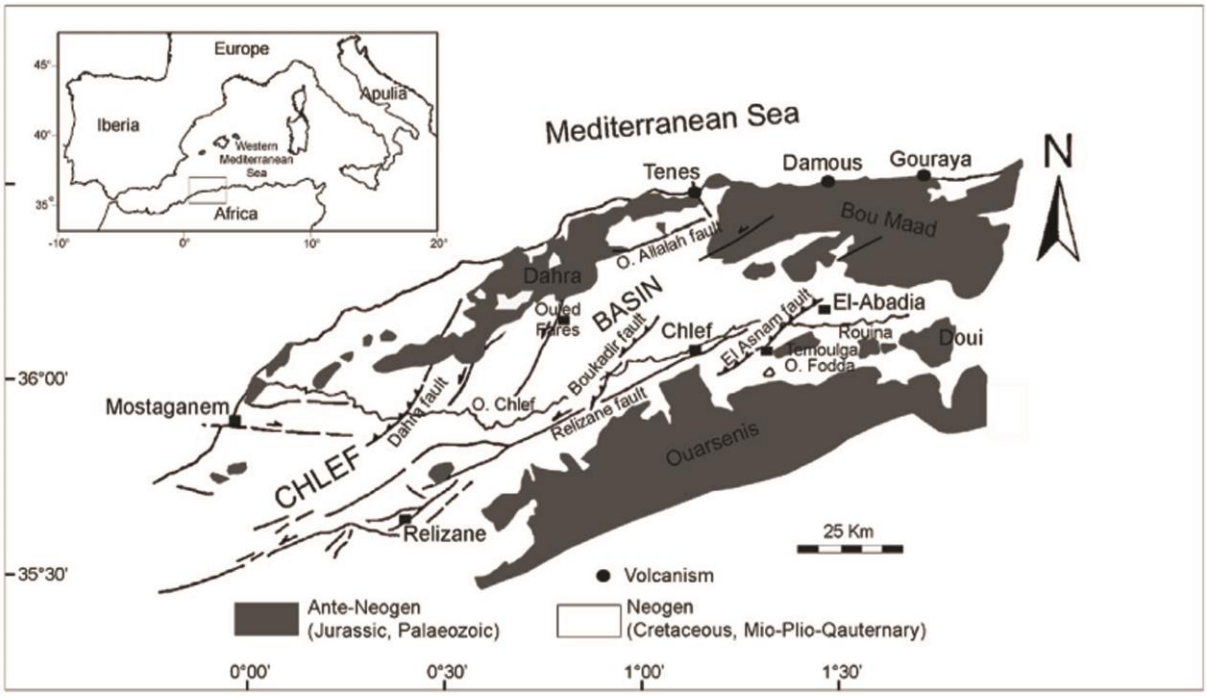

Figure 1. Geological map of the Chlef region (Modified from Meghraoui et al., 1986). The studied area (four-sided figure) is located in a box ranging from: 00°33'- 02°00'E in longitude and 35°48'-36°56'N in latitude.

ACCEPTED MANUSCRIPT

ACCEPTED MANUSCRIPT

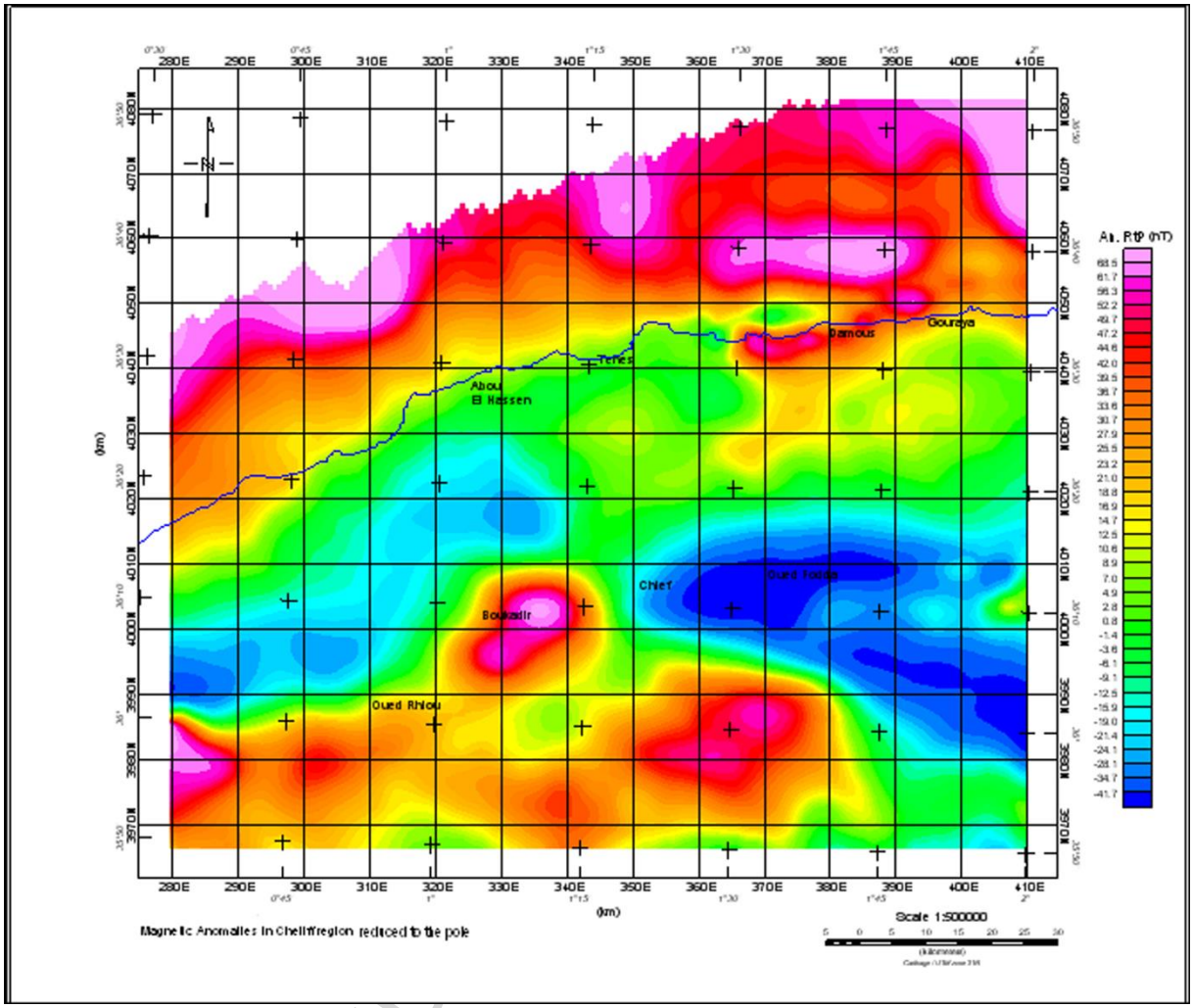

Figure 2. Aeromagnetic map of Chlef region: total field anomaly reduced to the pole.

ACCEPTED

ACCEPTED MANUSCRIPT

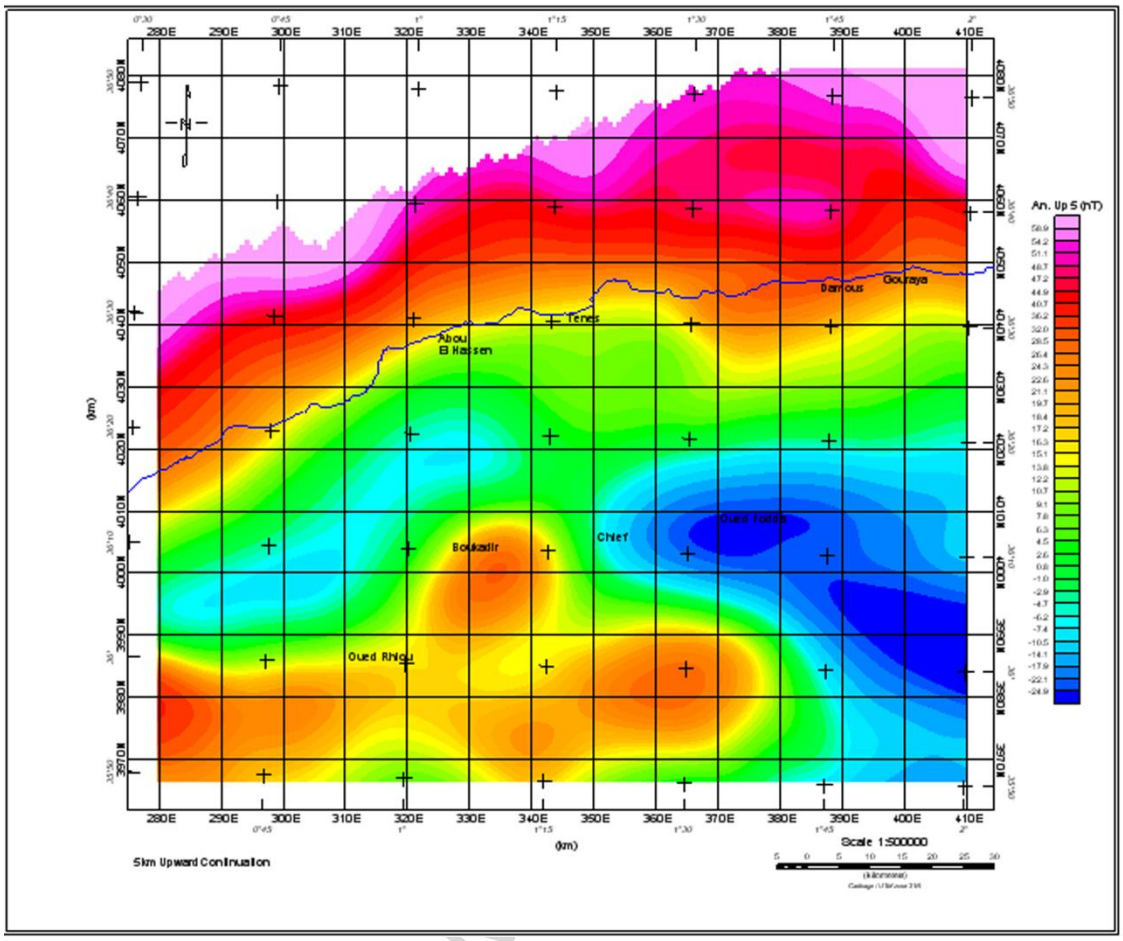

Figure 3. Aeromagnetic map of Chlef region: total field anomaly 5 km upward continued for showing long wavelengths.

ACCEPTED MANUSCRIPT

ACCEPTED MANUSCRIPT

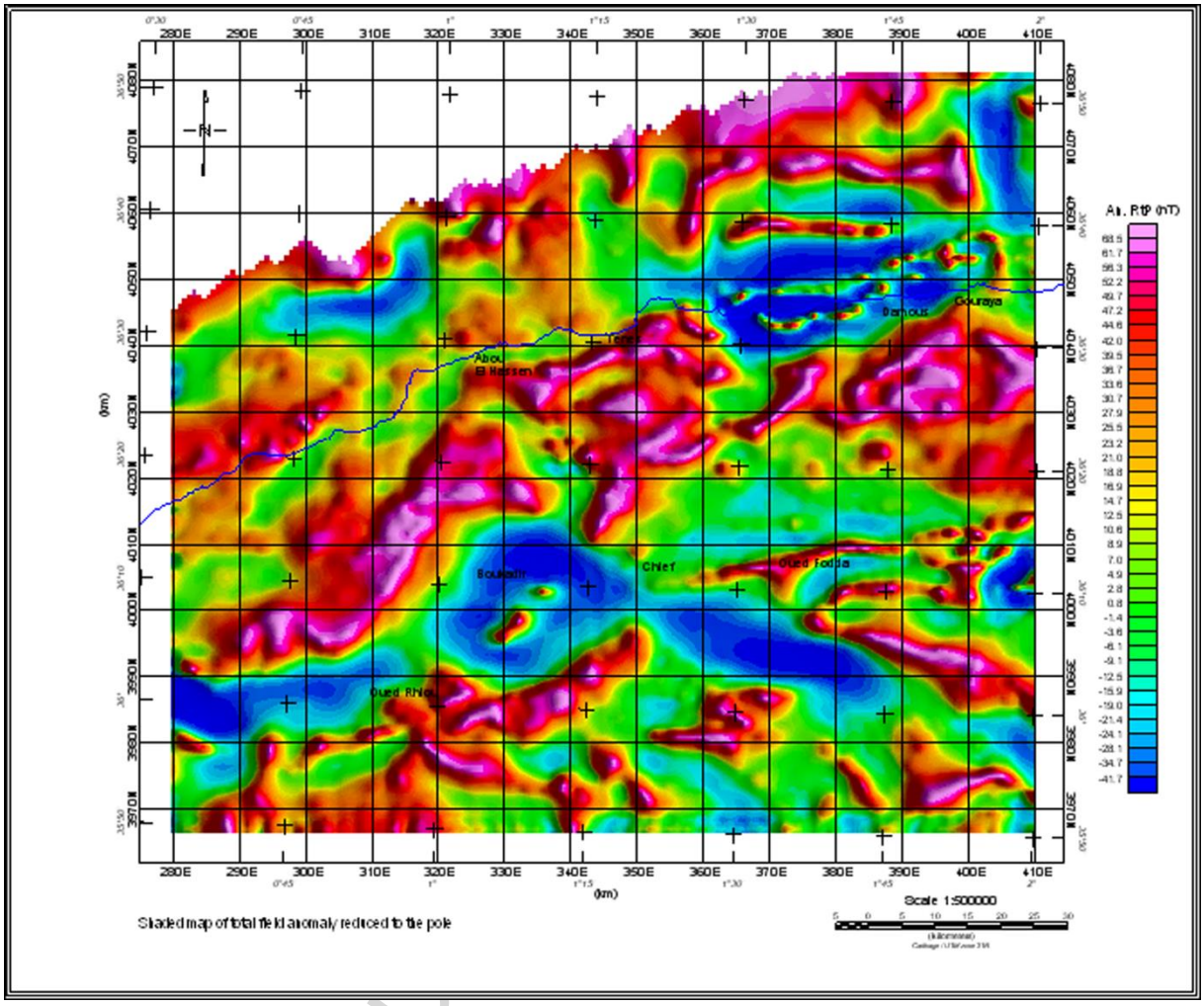

Figure 4. Aeromagnetic map of Chlef region: shaded map of total field anomaly reduced to the pole. This map allows seeing the magnetized structures and the correspondence with geological features.

ACCEPTED

ACCEPTED MANUSCRIPT

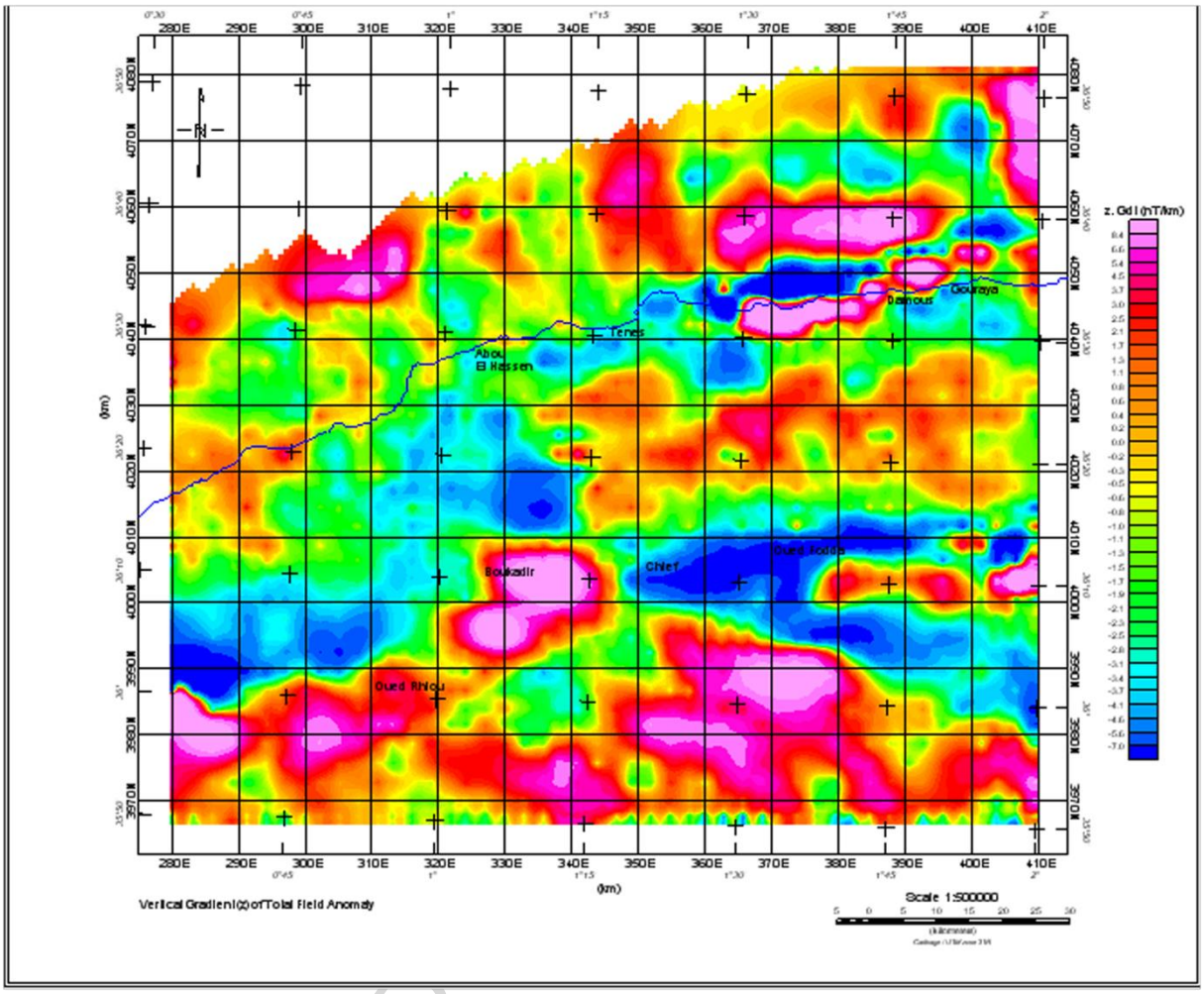

Figure 5. Aeromagnetic map of Chlef region: vertical gradient of the total field anomaly. Many magnetic lineaments appear corresponding to known and unknown geological contacts.

ACCEPTED

ACCEPTED MANUSCRIPT

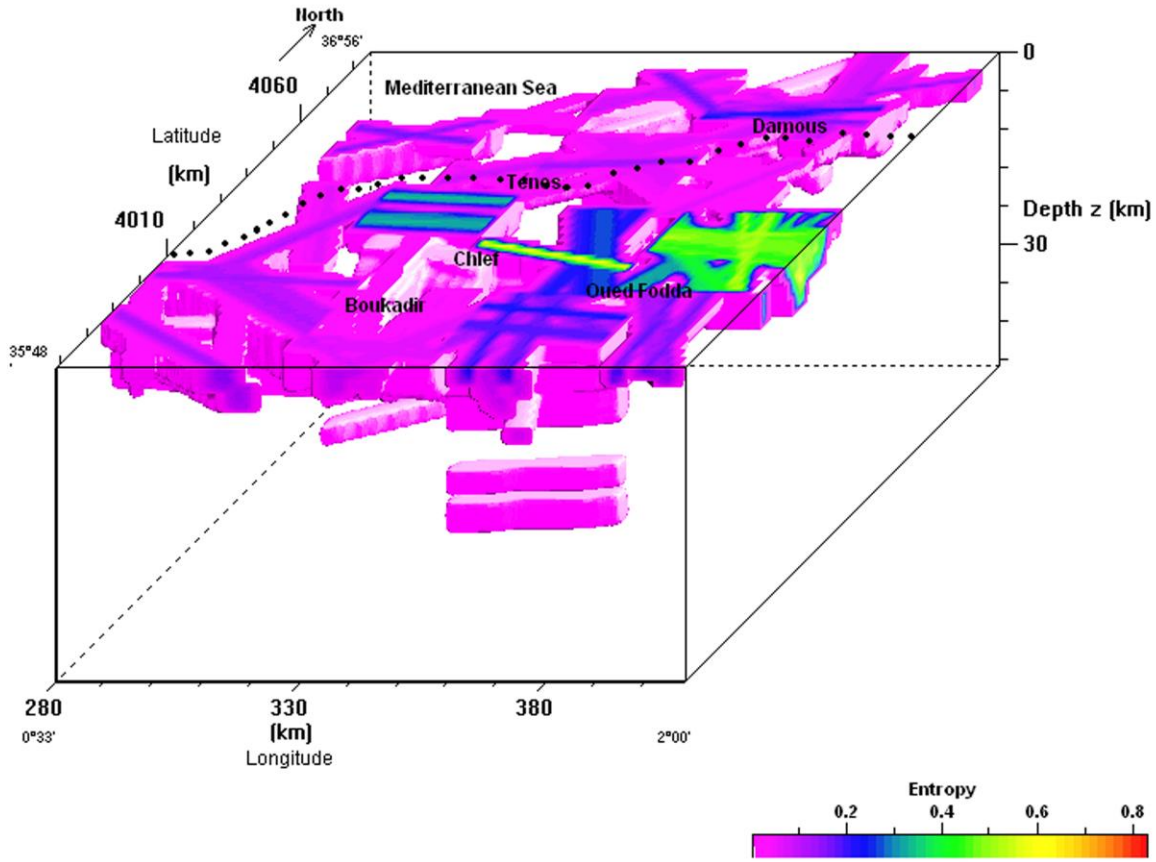

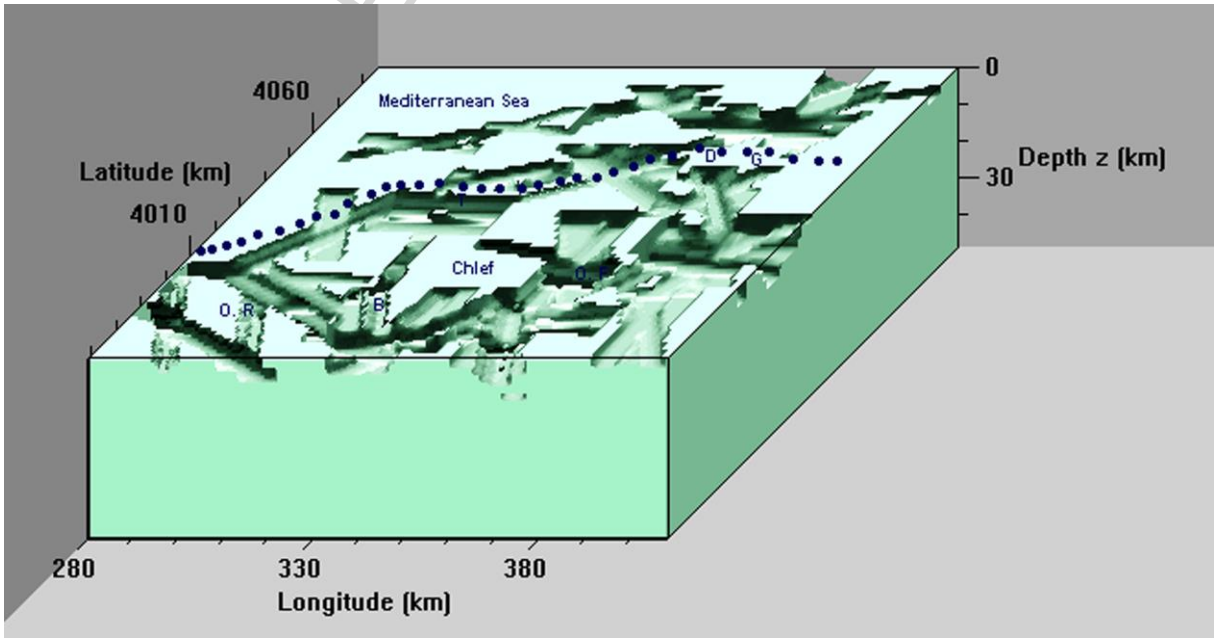

Figure 6. 3-D imaging of magnetized structures identified from the wavelet and ridgelet transforms (top) and their locations in the crust (bottom). The North direction is given

ACCEPTED MANUSCRIPT

by the latitude axis. The colour scale corresponds to the maximum entropy criteria (Tass et al., 1998; Boukerbout et al., 2003; Boukerbout and Gibert, 2006; Sailhac et al., 2009) for selecting sources location. (G: Gouraya, D: Damous, O.F.: Oued Fodda, B: Boukadir, O.R.: Oued Rhiou).

ACCEPTED MANUSCRIPT

ACCEPTED MANUSCRIPT

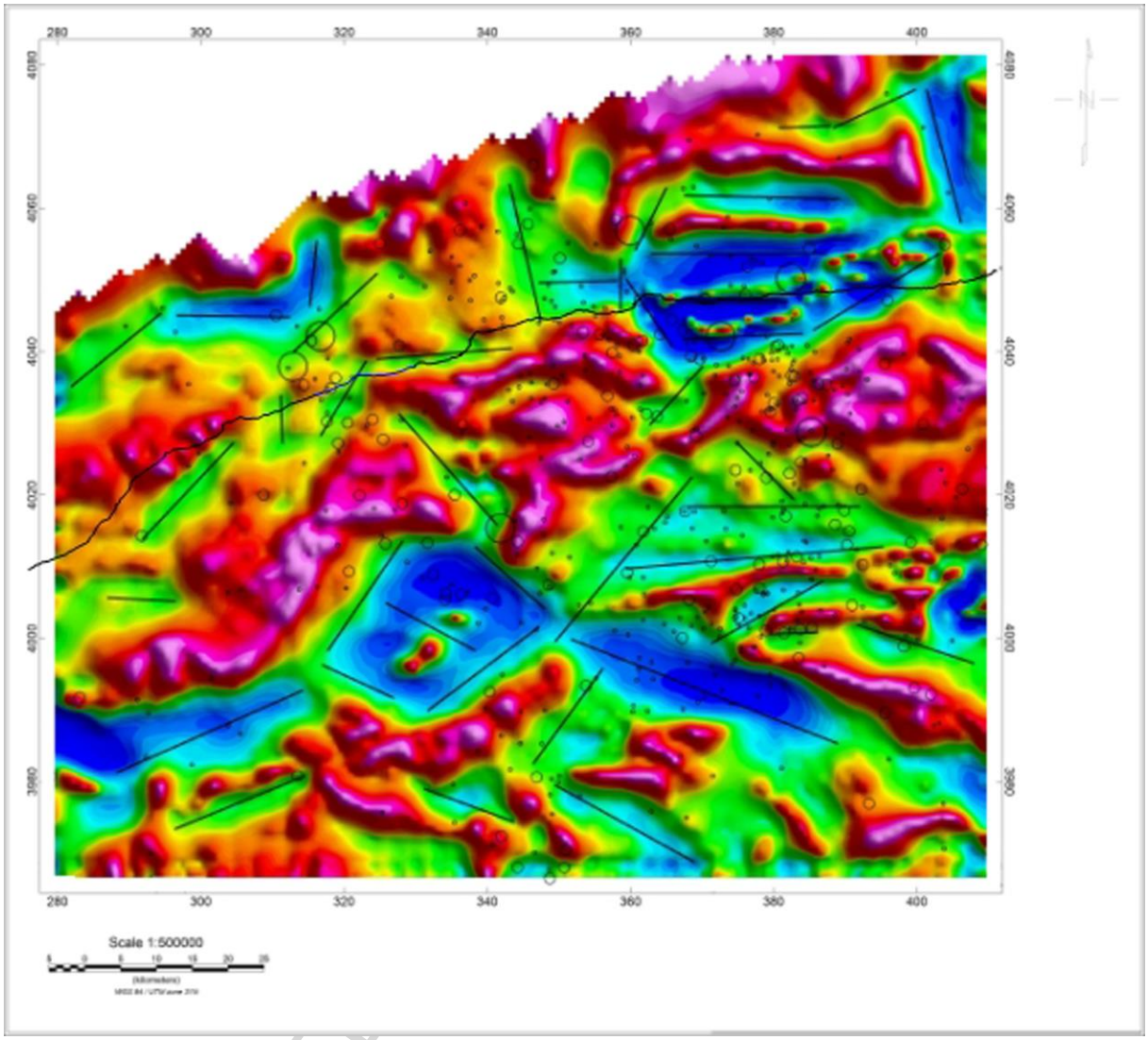

Figure 7. The compilation of identified magnetized features (black lines) from different analyzing methods reported on the shaded map and correlation with seismicity of the area (small, intermediate and big circles: 2<M<3, 3<M<4 and M>4).

ACCEPTED MANUSCRIPT

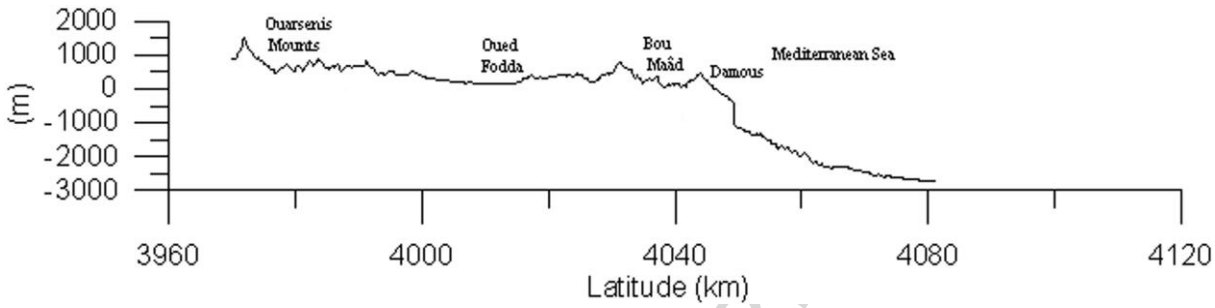

Figure 8 a. The topographic and bathymetric profile along the N-S aeromagnetic profile. The altitudes in this area vary from 500 to 1500m onshore and reach -2700m offshore.

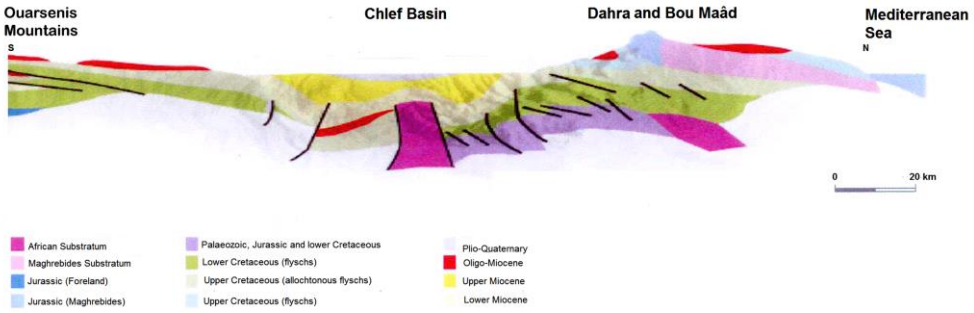

Figure 8 b. Structural cross-section along the N-S profile (Dahra-Bou Maad, Chlef basin, Ouarsenis Mountains) outlining folds and accidents (Modified from Megartsi, 1996).

ACCEPTED MANUSCRIPT

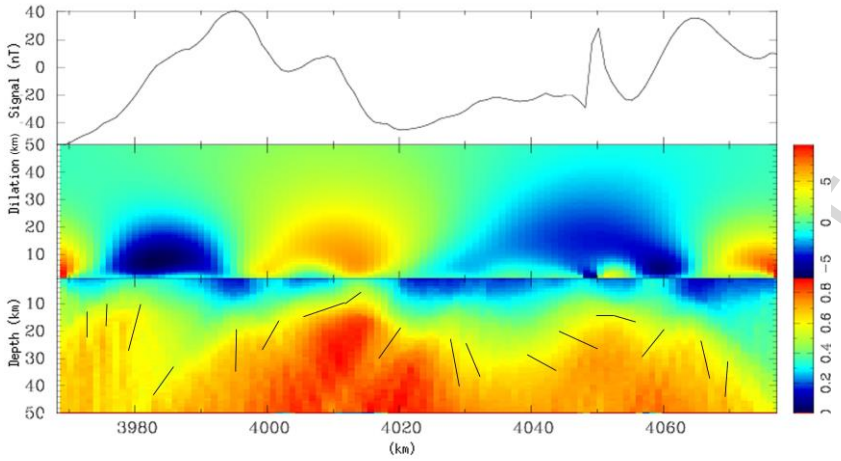

Figure 8 c. Identification of the magnetized substratum along the N-S profile using the modulus of continuous wavelet transform. The intensity of the magnetic anomaly (top) varies from -45 to +40nT.

The modulus of the continuous wavelet transform (middle) shows the signature of many contacts or faults. The depth (bottom) of the identified magnetized structures along this profile using the maximum entropy criteria is ranging between 6 and 30km. The deepest magnetized structures are located in the Ouarsenis Mounts (in the South) area and along the coast and in the Mediterranean Sea (in the North).

ACCEPTED MANUSCRIPT

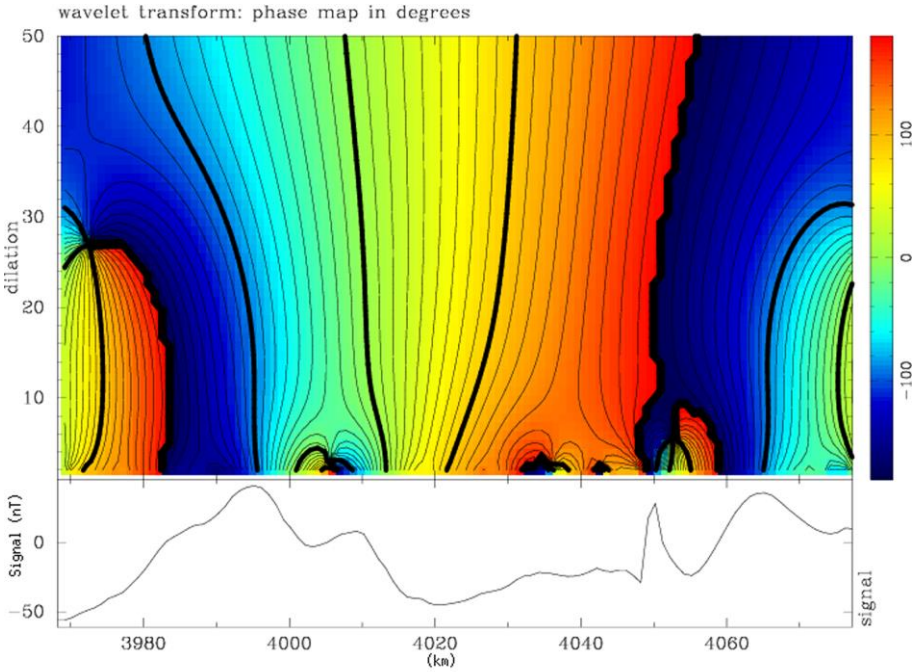

Figure 8 d. The phase of the wavelet transform gives the inclination of the identified contacts.

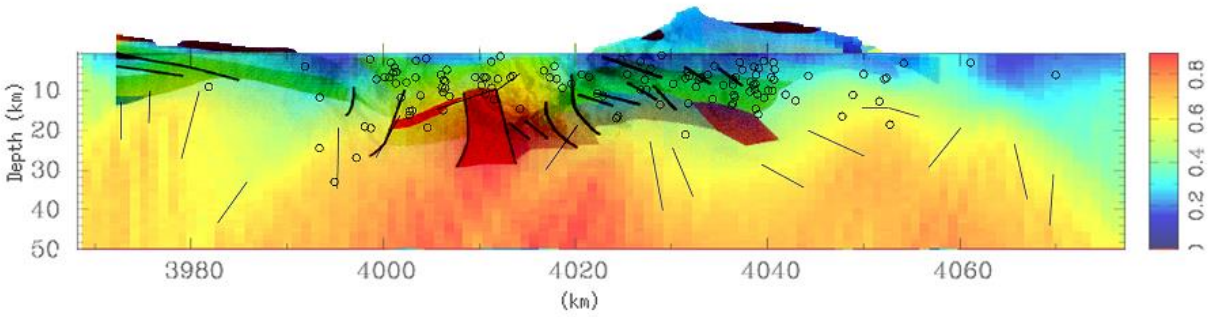

Figure 8 e. Correlation between identified structures with the continuous wavelet transform, the seismicity along the profile and the structural cross-section.

ACCEPTED MANUSCRIPT

Highlights

An aeromagnetic study of the seismically Chlef region is achieved.

Different processing methods are used to highlight short and long wavelengths.

The deep E-W structures limiting the area are identified.

2-D and 3-D images of emerging and deep structures both onshore and offshore are done.

A correlation between geology, seismicity and identified structures is done.

ACCEPTED MANUSCRIPT